#301

OGO-6

PLANAR ION TRAP

ION DENSITY, FLUX + TEMP. SUMMARIES

69-051A-03C

30 TAPES

Table of Contents

---

1. INTRODUCTION:

The documentation for this data set was originally on paper, kept in NSSDC's Data Set Catalogs (DSCs). The paper documentation in the Data Set Catalogs have been made into digital images, and then collected into a single PDF file for each Data Set Catalog. The inventory information in these DSCs is current as of July 1, 2004. This inventory information is now no longer maintained in the DSCs, but is now managed in the inventory part of the NSSDC information system. The information existing in the DSCs is now not needed for locating the data files, but we did not remove that inventory information.

The offline tape datasets have now been migrated from the original magnetic tape to Archival Information Packages (AIP's).

A prior restoration may have been done on data sets, if a requestor of this data set has questions; they should send an inquiry to the request office to see if additional information exists.

2. ERRATA/CHANGE LOG:

NOTE: Changes are made in a text box, and will show up that way when displayed on screen with a PDF reader.

When printing, special settings may be required to make the text box appear on the printed output.

Version	Date	Person	Page	Description of Change
01				
02				

3 LINKS TO RELEVANT INFORMATION IN THE ONLINE NSSDC INFORMATION SYSTEM:

http://nssdc.gsfc.nasa.gov/nmc/

[NOTE: This link will take you to the main page of the NSSDC Master Catalog. There you will be able to perform searches to find additional information]

4. CATALOG MATERIALS:

a. Associated Documents To find associated documents you will need to know the document ID number and then click here. http://nssdcftp.gsfc.nasa.gov/miscellaneous/documents/

b. Core Catalog Materials

OGO 6

ION DENSITY, FLUX & TEMP. SUMMARIES

69-051A-03C

SPIO-00055

THIS DATA SET HAS BEEN RESTORED. ORIGINALLY IT CONTAINED 30 9-TRACK, 800 BPI TAPES, WRITTEN IN BINARY, WITH THE EXCEPTION OF THE LAST TAPE, WHICH IS A BCD INDEX TAPE. THERE ARE FOUR RESTORED TAPES WRITTEN IN BINARY, WITH THE EXCEPTION OF THE LAST 29 FILES OF THE FOURTH TAPE (DR02520), WHICH IS WRITTEN IN EBCDIC. THE DR AND DS TAPES ARE 9-TRACK, 6250 BPI. THE ORIGINAL TAPES WERE CREATED ON AN IBM 360/75 COMPUTER. THE DR AND DS NUMBERS ALONG WITH THE CORRESPONDING D NUMBERS AND THE TIME SPANS ARE AS FOLLOWS:

DR#	DS#	D#	FILES	TIME SPAN
DR02502	DS02502	D20504	1	06/07/69 - 08/01/69
		D20503	2	08/01/69 - 08/15/69
		D20502	3	08/16/69 - 08/30/69
		D20501	4	08/30/69 - 10/10/69
		D20500	5	10/10/69 - 10/20/69
		D20499	6	10/20/69 - 10/29/69
		D20498	7	10/29/69 - 11/08/69
		D20497	8	11/08/69 - 11/20/69
		D20496	9	11/20/69 - 12/01/69
		D20495	10	12/01/69 - 12/11/69
		D20510	11	12/11/69 - 12/21/69
		D20511	12	12/21/69 - 12/31/69
		D20512	13	12/31/69 - 01/11/70
DR02503	DS02503	D20513	1	01/11/70 - 01/23/70
		D20514	2	01/23/70 - 02/05/70
		D20505	3	02/05/70 - 02/21/70
		D20506	4	02/21/70 - 03/08/70
		D20507	5	03/08/70 - 04/01/70
		D20508	6	04/01/70 - 04/15/70

DR#	DS#	D#	FILES	TIME SPAN
DR02504	DS02504	D20509	1	04/15/70 - 04/29/70
		D20515	2	04/29/70 - 05/10/70
		D20516	3	05/10/70 - 05/24/70
		D20517	4	05/24/70 - 07/11/70
		D20518	5	07/11/70 - 07/24/70
		D20519	6	07/24/70 - 08/06/70
DR02520	DS02520	D20520	1	08/06/70 - 08/26/70
		D20521	2	10/03/70 - 11/21/70
		D20522	3	11/21/70 - 01/27/71
		D20523	4	01/27/71 - 04/23/71
		D20524	5-33	06/07/69 - 04/23/71

REQ. AGENT	RAND NO.	ACQ. AGENT
CMT	RC3207	LLD
ROP	RC4167	

OGO-6

PLANAR ION TRAP

ION DENSITY, FLUX & TEMP. SUMMARIES

69-051A-03C

This data set consists of 30 data tapes and 1 Index tape. The data tapes are 800 BPI, Binary, 9-track, and have 1 file. The Index tape is 800 ~~BCD~~ EBCDIC, even, 9-track, and has 29 files. The tapes were created on an IBM 360/75 computer. The time spans are as follows:

D#	C#	ORBITS	TIME SPAN
D-20504	C-16933	20 - 814	06/07/69 - 08/01/69
D-20503	C-16934	815 - 1031	08/01/69 - 08/15/69
D-20502	C-16935	1032 - 1242	08/16/69 - 08/30/69
D-20501	C-16936	1243 - 1839	08/30/69 - 10/10/69
D-20500	C-16937	1840 - 1979	10/10/69 - 10/20/69
D-20499	C-16938	1980 - 2115	10/20/69 - 10/29/69
D-20498	C-16939	2116 - 2259	10/29/69 - 11/08/69
D-20497	C-16940	2260 - 2423	11/08/69 - 11/20/69
D-20496	C-16941	2424 - 2582	11/20/69 - 12/01/69
D-20495	C-16942	2583 - 2727	12/01/69 - 12/11/69
D-20510	C-16943	2728 - 2878	12/11/69 - 12/21/69
D-20511	C-16944	2879 - 3013	12/21/69 - 12/31/69
D-20512	C-16945	3014 - 3183	12/31/69 - 01/11/70
D-20513	C-16946	3184 - 3358	01/11/70 - 01/23/70
D-20514	C-16947	3359 - 3542	01/23/70 - 02/05/70
D-20505	C-16948	3543 - 3771	02/05/70 - 02/21/70
D-20506	C-16949	3771 - 3989	02/21/70 - 03/08/70

D#	C#	ORBITS	TIME SPAN
D-20507	C-16950	3990 - 4334	03/08/70 - 04/01/70
D-20508	C-16951	4335 - 4549	04/01/70 - 04/15/70
D-20509	C-16952	4550 - 4739	04/15/70 - 04/29/70
D-20515	C-16953	4740 - 4905	04/29/70 - 05/10/70
D-20516	C-16954	4906 - 5114	05/10/70 -05/24/70
D-20517	C-16955	5115 - 5803	05/24/70 - 07/11/70
D-20518	C-16956	5804 - 5989	07/11/70 - 07/24/70
D-20519	C-16957	5990 - 6176	07/24/70 - 08/06/70
D-20520	C-16958	6177 - 6476	08/06/70 - 08/26/70
D-20521	C-16959	7020 - 7738	10/03/70 - 11/21/70
D-20522	C-16960	7739 - 8719	11/21/70 - 01/27/71
D-20523	C-16961	8720 - 9978	01/27/71 - 04/23/71
D-20524	C-16962	20 - 9978	06/07/69 - 04/23/71

MAGNETIC TAPE DESCRIPTION
OGO-6 F-03 Retarding Potential Analyzer

Dr. W. B. Hanson
The University of Texas at Dallas

The magnetic tapes are unlabeled 9-track, 800 bpi and odd parity. Each magnetic tape consists of one file of fixed length physical records which are 3168 bytes (792 words) long. Each physical record contains 12 fixed length logical records which are 264 bytes (66 words) long. The last physical record is normally short.

There will be a total of approximately 30 35 magnetic tapes, each consisting of approximately 2200 feet (approximately 5600 physical records; 67200 logical records) of information. The information on these magnetic tapes is strictly chronological and contains no overlapping information; orbits are not split across magnetic tape boundaries.

For each magnetic tape, there is a printed summary giving each orbit number; the logical record number in which that orbit started; the year, day and time information started in that orbit; the year, day and time information stopped in that orbit; and a summary of sweeps for that orbit (S/N implies slow sweeps which were not analyzed; F/N implies fast sweeps which were not analyzed; S/A implies slow sweeps which were analyzed; F/A implies fast sweeps which were analyzed; ALL implies total sweeps).

A description and units for each word in the logical record is shown on the attached logical record layout. Some of the items will be further delineated.

OGO VI RPA DATA

OGO VI was launched on June 5, 1969 into an 82^{o} inclination prograde orbit, with nominal apogee and perigee of 1100 km and 400 km. The initial orbit plane was in a near dawn-dusk configuration, and it rotated approximately two degrees local time each day. After nearly two weeks of normal operation a malfunction in the solar power system caused the vehicle potential, ψ_s, to have a large negative value ($|\psi_s| > 20$ volts) when the spacecraft was sunlit. Subsequently, the daytime magnitude of ψ_s changed discontinuously on several occasions, and during late 1969 and early 1970 it did not exceed 14 volts. Gradually the vehicle system lost capability and it became increasingly unreliable to read out the tape recorders. The spacecraft was finally turned off as a fiscal expediency in late 1971, with several of its instruments, including the Retarding Potential Analyzer, still in perfect working order.

OGO VI proved to be an excellent scientific spacecraft. It provided in excess of 5000 complete orbits of data during its lifetime. The principal devices that supplied aeronomical data were the RPA, a neutral mass spectrometer, a Bennett ion mass spectrometer, a single axis electric field experiment, 6300 A and 5577 A airglow photometers, and a 6300 A interferometer for measuring the neutral atmospheric temperature. Some langmuir probe data are also available, as are some energetic particle data ($E > 20$ Kev), and some electromagnetic wave intensity data over wide frequency ranges. Very limited syntheses of data from the various instruments have been carried out to date.

The RPA data that is available in the World Data Center comprises nearly all the data that could be analyzed for ion temperature. In addition, much more data is included that provides an irregularity index for the total ion concentration, N_i, as well as a parameter that closely characterizes N_i itself. During the first 240 orbits when ψ_s was well behaved the ion temperature was measured over the complete orbits. After ψ_s became large in sunlight the Retarding Potential could no longer repell ions from the collector and current voltage characteristic curves could not be obtained except when the spacecraft was in eclipse. During a four month period at the end of 1969 and the beginning of 1970 $|\psi_s|$ decreased to below 14 volts and it was possible to analyze the sunlit data for T_i, and for H^+, He^+, and O^+ ion concentrations. We call this "good-bad" data; it is of variable quality, but always less reliable than the sunlit data from orbit numbers less than 240. Not all of the "good-bad" daytime data was analyzed.

The RPA data appears in three different plot forms, only two of which exist for all the data analyzed, and only these two are available from the World Data Center. All of the data in these two summary film plots, called SAT plots and Sigma plots, are also available on a set of 30 800 bpi magnetic tapes. The other plot format, called OGO plots, is a plot of the individual ion characteristic curves and the essentially raw irregularity data. This primary data plot format was essential for developing confidence in the data analysis techniques employed and for resolving questions that arise from peculiar behavior observed in the summary data plots. Many such questions continue to arise as we examine new summary data, but unfortunately OGO plots do not exist for most of the data because of economic considerations.

Any prospective user of the RPA data would be well advised to examine at least one roll of OGO plot film in order to obtain a feel for the raw data, and for the curve fitting that provides most of the summary plot numbers.

OGO 6 RPA BIBLIOGRAPHY

"Plasma Measurements with the Retarding Potential Analyser on OGO VI," with S. Sanatani, D. Zuccaro, and T. W. Flowerday, J. Geophys. Res., 75 (28), 5483, 1970

"Meteoric Ions above the F_2 Peak," with S. Sanatani, J. Geophys. Res., 75 (28), 5503, 1970

"The Relationship between Fe^+ Ions and Equatorial Spread F," with S. Sanatani, J. Geophys. Res. 76, 7761, 1971

"Errors in Retarding Potential Analyzers Caused by Nonuniformity of the Grid Plane Potential," with D. R. Frame and J. E. Midgley, J. Geophys. Res. 77, 1914, 1972

"Molecular Ions in the F2 Layer," with H. Rishbeth and P. Bauer, Planet. Space Sci. 20, 1287, 1972

"Satellite and Ground Based Observations of a Red Arc," with A. F. Nagy, T. L. Aggson and R. J. Hoch, J. Geophys. Res. 77, 3613, 1972

"The Source and Identification of Heavy Ions in the Equatorial F Layer," with D. L. Sterling and R. F. Woodman, J. Geophys. Res. 77, 5530, 1972

"Comparison of T_e and T_i from OGO 6 and from Various Incoherent Scatter Radars," with J. P. McClure, A. F. Nagy, R. J. Cicerone, L. H. Brace, M. Baron, P. Bauer, H. C. Carlson, J. V. Evans, G. N. Taylor, and R. F. Woodman, J. Geophys. Res. 78, 197, 1973

"OGO-6 Measurements of Supercooled Plasma in the Equatorial Exosphere," with A. F. Nagy and R. J. Moffett, J. Geophys. Res. 78, 751, 1973

"Large N_i Gradients Below the Equatorial F Peak," with S. Sanatani, J. Geophys. Res. 78, 1157, 1973

"On the Cause of Equatorial Spread F," with J. P. McClure and D. L. Sterling, J. Geophys. Res. 78, 2353, 1973

"Effects of Interhemisphere Transport on Plasma Temperatures at Low Latitudes," with G. J. Bailey, R. J. Moffett and S. Sanatani, J. Geophys. Res. 78, 5597, 1973

"A Catalog of Ionospheric F Region Irregularity Behavior Based on Ogo 6 Retarding Potential Analyzer Data," with J. P. McClure, J. Geophys. Res. 78, 7431, 1973

"In Situ Measurements of the Spectral Characteristics of F Region Ionospheric Irregularities," with P. L. Dyson and J. P. McClure, J. Geophys. Res. 79, 1497, 1974

SUMMARY OF MAGNETIC TAPE FORMATION

OGO-6 F-03 Retarding Potential Analyzer

Dr. W. B. Hanson
The University of Texas at Dallas

Tape Number	Started				Stopped			
	Orbit	Year	Day	Time	Orbit	Year	Day	Time
WDB001	20	1969	158	2825	814	1969	213	796
WDB002	815	1969	213	1635	1031	1969	227	83279
WDB003	1032	1969	228	3594	1242	1969	242	53655
WDB004	1243	1969	242	53665	1839	1969	283	78824
WDB005	1840	1969	283	78833	1979	1969	293	51020
WDB006	1980	1969	293	51029	2115	1969	302	85521
WDB007	2116	1969	302	85531	2259	1969	312	81220
WDB008	2260	1969	312	81229	2423	1969	324	23373
WDB009	2424	1969	324	23382	2582	1969	335	21940
WDB010	2583	1969	335	21950	2727	1969	345	23198
WDB011	2728	1969	345	23208	2878	1969	355	60171
DB012	2879	1969	355	60180	3013	1969	365	1594
WDB013	3014	1969	365	1603	3183	1970	011	65349
WDB014	3184	1970	011	65359	3358	1970	023	72426
WDB015	3359	1970	023	72435	3542	1970	036	46585
WDB016	3543	1970	036	46595	3770	1970	052	23616
WDB017	3771	1970	052	23625	3989	1970	067	32886
WDB018	3990	1970	067	32895	4334	1970	091	14919
WDB019	4335	1970	091	14929	4549	1970	105	86114
WDB020	4550	1970	105	86124	4739	1970	119	4014
WDB021	4740	1970	119	9200	4905	1970	130	46005
WDB022	4906	1970	130	46015	5114	1970	144	79678
WDB023	5115	1970	144	82060	5803	1970	192	31179
WDB024	5804	1970	192	31189	5989	1970	205	13591
WDB025	5990	1970	205	13600	6176	1970	218	1691
WDB026	6177	1970	218	1700	6476	1970	238	56263
WDB027	7020	1970	276	392	7738	1970	325	31024
DB028	7739	1970	325	33644	8719	1971	027	59359
WDB029	8720	1971	027	59368	9978	1971	113	80041
WDB030	INDEX							

Logical Record Layout

OGO-6 F-03 Retarding Potential Analyzer

Word		Description	Units
01	I	Tape Number	1,2,...
02	I	Record Number	1,2,...
03	I	Meaningful Words in Record	47,66
04	I	Orbit Number	20,21,...,9978
05	I	Gregorian Year	Year
06	I	Julian Day of Year	Days
07	I	Second of the Day (GMT)	Seconds
08	I	Local Apparent Solar Time	Hours
09	I	Local Apparent Solar Time	Minutes
10	I	Local Apparent Solar Time	Seconds
11	R	Satellite Altitude	Km
12	R	Satellite Velocity	Km/Second
13	I	Satellite Sunlit Flag (1 => Sunlit)	0,1
14	R	Geodetic Latitude	Degrees (± 90)
15	R	Geodetic Longitude	Degrees (±180)
16	R	Attack Angle	Degrees
17	R	Sun Angle	Degrees (± 90)
18	R	Zenith Angle	Degrees
19	R	North Height	Km
20	R	South Height	Km
21	R	Egress Geodetic Latitude	Degrees (± 90)
22	R	Egress Geodetic Longitude	Degrees (±180)
23	R	Ingress Geodetic Latitude	Degrees (± 90)
24	R	Ingress Geodetic Longitude	Degrees (±180)
25	R	Geomagnetic Dip Angle	Degrees (± 90)
26	R	Dip Latitude	Degrees (± 90)
27	R	Dipole Latitude	Degrees (± 90)
28	R	Geomagnetic Field Strength	Gauss
29	R	McIlwain Shell Parameter	Earth Radii -
30	I	Sweep Number	1,2,...
31	I	Fast/Slow Sweep Mode Flag (1 => Fast)	0,1
32	I	Normal/Abnormal Sweep Flag (1 => Normal)	0,1
33	R	Trap Mode Start Time	Seconds
34	R	Trap Mode Period	Seconds
35	I	Electrometer Range at Saturation	1,2,...,8
36	R	Trap Mode Sweep Slope	Volts/Second
37	R	Plasma Drift Velocity	Km/Second
38	R	Suprathermal Electron Current	Amps
39	R	Electron Flux	#/Cm²/Second
40	R	Total Ion Current at Saturation	Amps
41	R	Duct Mode Start Time	Seconds
42	R	Duct Mode Period	Seconds
43	R	Duct Mode Starting Electrometer Voltage	Volts
44	R	Total Ion Concentration Deviations	% (Filler=999.0)
45	R	Offset Duct Mode Start Time	Seconds
46	R	Offset Duct Mode Starting Electrometer Voltage	Volts
47	I	Offset Duct Mode Starting Electrometer Range	1,2,...,8
48	I	Number of Ions in Least Squares Analysis	1,2,...,5
49	R	Standard Deviation of Least Squares Analysis	%
50	R	Ion Temperature	Degrees Kelvin
51	R	Satellite Potential	Volts
52	R	Plasma Drift Velocity	Km/Second
53	R	Ion Concentration - 1+	#/Cm³
54	R	Ion Concentration - 4+	#/Cm³
55	R	Ion Concentration - 16+	#/Cm³
56	R	Ion Concentration - 30+	#/Cm³
57	R	Ion Concentration - 56+	#/Cm³
58	R	Ion Concentration - Total	#/Cm³
59	R	Error - Ion Temperature	Degrees Kelvin
60	R	Error - Satellite Potential	Volts
61	R	Error - Plasma Drift Velocity	Km/Second
62	R	Error - 1+	#/Cm³
63	R	Error - 4+	#/Cm³
64	R	Error - 16+	#/Cm³
65	R	Error - 30+	#/Cm³
66	R	Error - 56+	#/Cm³

The information is in the internal format for IBM 360/370 computers. Information is full word binary fixed point denoted by I or is full word hexadecimal floating point denoted by R.

OGO 6 Ion Concentration and Ion Irregularity Data

W. B. Hanson

The Retarding Potential Analyzer Data from OGO 6 constitute the only proven reservoir of satellite ion temperature data prior to Atmosphere Explorer. Similarly, the most sensitive and comprehensive body of data on ionospheric irregularities is available from the same instrument. Because of the unique nature and excellent quality of these results it is important to have the data reduced to useful forms and to have it generally available.

The data analysis and presentations have been refined over a period of years and the data bank has now been completely processed, insofar as this seems fiscally responsible. All of the data output has now been summarized on 30 magnetic tapes and several rolls of microfilm in different formats. These are now in the process of being sent to the NASA World Data Center. With the completion of this effort we can now examine the large body of data in an orderly manner for morphological characteristics, as well as make comparisons with data from other OGO 6 measurements.

A rather elaborate data key has been written to supplement the magnetic tape and film that are being shipped to the World Data Center. The description of the tapes fills a volume that is too large to append here, but the summary page for the tapes and a description of the data included are attached. The film description is more modest and has been appended in its entirety.

RPA SAT PLOTS

Each frame of these plots displays a set of reduced RPA data acquired between $\pm 82°$ geographic latitude. The quantities plotted are ion temperature, ion concentrations and electron fluxes. Several orbital parameters are printed out at the bottom, and the dip latitude at which these values apply are indicated by tic marks on both the top and bottom scales.

The density of points plotted is variable and depends on the mode of the instrument, the quality of the telemetry data, the variation of dip latitude with time, and the fraction of data properly analyzed. Bad data fits* are rejected by an arbitrary criterion; if the mean square deviation of the experimental points from the theoretical curve is > 10% the N_i and T_i values shown in OGO PLOTS are not plotted in SAT PLOTS. This criterion is not perfect and occasionally values are plotted which are obviously incorrect, usually because of an electrometer ranging error. In these cases the major ion concentrations will appear a factor of $(10)^{n/2}$ above or below the correct value.

The ion temperature values are plotted as a small dot with a vertical bar centered on this dot whose length corresponds to the statistical error in T_i. Much of the time these error bars lie entirely within the dots. Three different temperature scales are available, 500 K to 2000 K, 500 K to 3500 K, and 0 K to 6000 K. The appropriate scale is determined by an algorithm that examines the data set to be plotted.

The "photo-flux" values at the bottom of the T_i plots correspond to electron fluxes of energy greater than 10 ev, unless Fe^+ is present.

*See OGO plots discussion

In the latter case the plotted values are nearly proportional to the Fe^+ concentration. We cannot simultaneously determine both an electron flux and the Fe^+ concentration. Usually this is no problem since Fe^+ is confined to dip latitudes < $\pm 30°$ and conjugate photo electrons and auroral electrons generally occur at higher latitudes. In the daytime, photoelectrons mask the presence of Fe^+.

The magnitude of the electron flux is obtained by dividing the negative current to the collector by the effective area of the aperture (i.e., including grid transmission). The flux is then 2.9×10^6 cm^{-2} sec^{-1} per bit (1 bit $\approx 6 \times 10^{-13}$ amps). A full geometrical calculation shows that for an isotropic maxwellian photoelectron gas with a temperature of 7 ev, the ambient flux above 10 ev (+ spacecraft potential) is approximately 10^6 electrons/cm^2 sec ster bit.

The zero level of the electrometer drifts between the zero and 3 bit levels though the noise level is small compared to one bit. Most of the data plotted has been corrected for this effect, except when Fe^+ is present. Unfortunately, some of the plots erroneously show the zero level plotted as an electron flux.

The derivation of the various ion concentrations assumes that the plasma is at rest in the earth's frame of reference, and that the molecular ions have a mass of 30 AMU. Often this leads to an incorrect ratio of (H^+/He^+) ions near the equator when the inter-hemisphere plasma velocity is large. This same plasma motion causes the derived values of T_i to be too large or too small, depending on

whether the plasma motion is toward or away from the satellite, respectively.

The statistical errors in T_i are normally quite small when $n(O^+) > 10^3$ cm^{-3}, but if the Stanford antenna on the spacecraft is being positively biased in pulses a periodic structure in T_i can be observed, whose amplitude is rather larger than the error bars. These are not real changes in T_i induced by the transmitter, but faulty ion curves distorted by the antenna pulses. This condition can only be confirmed by examining the OGO plots. Orbit numbers 3029 to 8330 were flown in 1970; smaller orbit numbers refer to 1969 and larger numbers to 1971. New orbits are commenced when the satellite traverses the equatorial plane from South to North.

On some orbits the OPEP (orbital plane experimental package) on which the RPA is mounted is scanned continuously through ram and into the wake and back again. The data from these orbits is not very useful, but is easily recognized by the periodic disappearance of the plasma. The values taken near the ram have some validity if taken in the fast mode.

Definition of Parameters

ALT - satellite altitude in km

LNG - geographic longitude

LAT - geographic latitude

LT - local time in hours and minutes

DIP - magnetic dip angle in degrees

Z - solar zenith angle in degrees

NH - solid earth (solar) screening height at north conjugate point

SH - solid earth (solar) screening height at south conjugate point

L - McIlwain L parameter

SA - angle between normal to sensor face and the sun

UT - universal time in seconds of the day

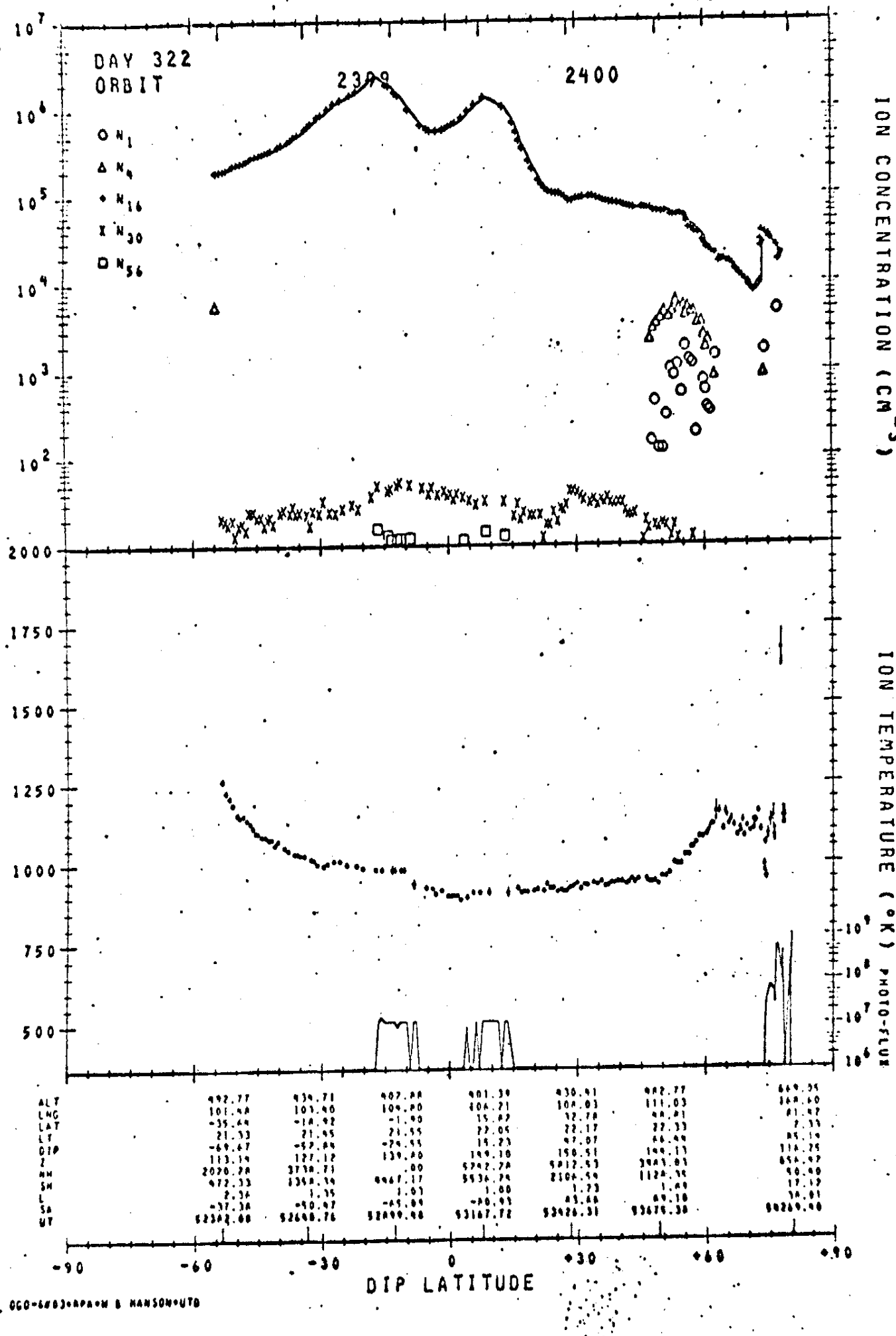

OGO-6/OV3-4/PA+M B HANSON+UTD

RPA SIGMA PLOTS

Each frame of SIGMA PLOTS displays up to 60 minutes of reduced Ogo 6 RPA data, starting at middle latitudes ($\Lambda \geq +35°$ or $\leq -35°$) and crossing the polar cap and the subsequent middle, low and middle latitude regions. The quantities plotted are the total ion (electron) concentration, the ionospheric irregularity index ($\Sigma = \Delta N_i/N_i$, RMS%), the satellite altitude, the altitude of the earth's shadow at the northern and southern end of the satellite's geomagnetic field tube, the size of the ionospheric irregularities (km/peak), and, where available, the ion temperature, the ion concentrations $[16^+]$, $[30^+]$, $[56^+]$ and $[4^+ + 1^+]$, and the photoelectron flux. These latter parameters (temperature, ion composition data and flux) are usually available only during satellite eclipse.

Blocks of orbital parameters are provided at the bottom, and the dip latitudes where these data blocks apply (2 to 10 data blocks are provided) are indicated by the numbers 1 through 10 shown on the lower scale. Parameters provided are invariant latitude, magnetic dipole local time, local time, longitude, latitude, solar zenith angle, sun angle (angle between the sun and the normal to the RPA aperture plane), universal time, and satellite altitude.

The polar plot in the lower left corner gives the value of $\Sigma(\Delta N_i/N_i$, RMS%) versus invariant latitude and dipole local time along the satellite track. The smallest dots indicate $\Sigma < 1\%$; the medium dots, $1\% < \Sigma < 10\%$; and the large dots, $\Sigma > 10\%$. The dots plotted are obtained from the 5-point running means, which are the circles connected by a heavy line on the plot at the top of the frame.

Just below the Σ plot the satellite altitude is indicated by the sinusoidal curve (perigee ∿400 km, apogee ∿1100 km). The symbols N and S give the altitude of the earth's geometrical shadow, assuming no screening by the earth's atmosphere, at the northern and southern intersection of the earth's surface and the geomagnetic field line through the satellite. The determination of these screening heights, which are significant for anticipating the presence of conjugate photoelectrons, is often faulty, but even the nonsense values have been plotted. Superimposed on the altitude plots is a plot of electron flux (cm^{-2} sec^{-1}) of energy greater than 10 ev, unless Fe^+ is present. In the latter case the plotted values are nearly proportional to the Fe^+ concentration. Because of a 20 volt limit on the retarding potential we cannot simultaneously determine both the electron flux and the Fe^+ concentration, but usually this is no problem because Fe^+ is observed only for dip latitudes < $\pm 30°$ and auroral electrons or conjugate photoelectrons generally occur only at higher latitudes.

The size parameter plotted next is of limited utility because of inadequacies in the algorithm used to calculate it. In particular, the upper limit occurring between 30 and 40 km is set by the distance the satellite travels during the fast "duct" or irregularity-measuring operation,* and has no geophysical significance.

Ion temperatures are plotted as a small dot with a vertical error bar whose length corresponds to the statistical error in T_i. These error bars often lie entirely within the dot. The density of T_i points plotted is variable, depending on the instrument mode, on the quality of the data and on the fraction of data properly interpreted by the analysis algorithms.

*See the OGO Plots write-up

Bad fits* are rejected by an arbitrary criterion: if the RMS deviation between the best-fitting theoretical curve and the experimental points exceeds 10%, the N_i and T_i values derived are not plotted. Occasional values are plotted which are obviously incorrect, usually because of an electrometer ranging error. In these cases N_i will be one or more factors of $\sqrt{10}$ above or below the correct value of N_i.

When the satellite is not in eclipse (and after orbit 240) the total N_i value and the Σ values can still be obtained, even though the (-) satellite potential is usually too large to measure T_i. The derived N_i, however, is somewhat larger than the ambient value, owing to the ion focussing of the very negative spacecraft. The magnitude of this overestimate is larger the greater the proportion of light ions (H^+ and He^+) present. Factors of order 2 are involved. From day 297/69 to day 055/70 it is still possible to deduce daytime T_i values, though with lower accuracy, because the satellite potential is smaller than 14 volts when the satellite is in sunlight during this period.

The total $N_i(N_e)$ value often shows a great deal of randomness when the satellite is not eclipsed because of faulty algorithms used for the determination of this quantity. Very often the eye can follow the actual changes in N_i, despite this weakness, but we apologize for this failure. Whether the satellite is or is not eclipsed, the derivation of the various ion concentrations assumes that the plasma is at rest in the earth's frame of reference, and that the molecular ions have a mass of 30 AMU. Often this leads to an incorrect ratio of (H^+/He^+) ions near the equator when the

*See the OGO Plots write-up

interhemisphere plasma velocity is large. This same plasma motion causes the derived values of both N_i and T_i to be too large or too small, depending on whether the plasma motion is toward or away from the satellite, respectively.

SIGMA 101

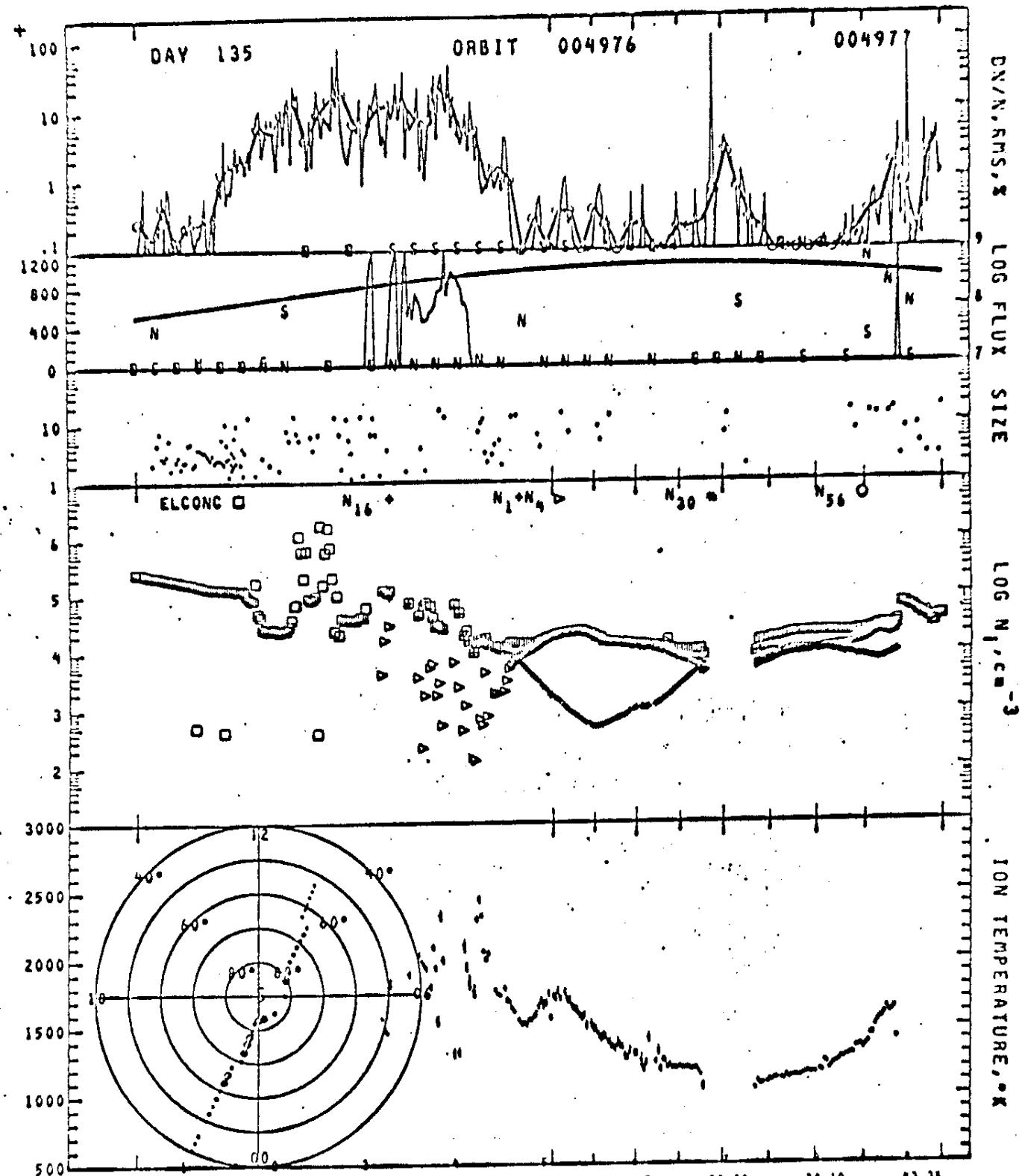

OGO-6#03•APA•W B HANSON•UTD

RPA OGO PLOTS

Each frame of this plot shows four separate data sequences, each having one "sweep" and one "duct" operation. The left hand side shows a logarithmic plot of ion current versus retarding potential, where the plotted points are experimental and the line is a theoretical fit to the data (see Hanson et al., 1970, for details). The right side contains the "duct" data and reveals the changes in ion concentration observed along the satellite flight path. Various geophysical coordinates are printed out between the data plots. Data can be recorded in either the fast or slow mode. In the fast mode the ion sweep and the duct operation each take approximately 5 seconds, whereas in the slow mode they are allotted 20 seconds each. So many points are plotted in the slow ion sweeps that one cannot usually see the theoretical curve plotted through them.

The derived values of ion temperature and ion concentrations are printed out in the middle for each sweep that is analyzed, together with their statistical error bars. Also given are the vehicle potential and σ, the mean square fractional deviation of the measured points from the least-squares best-fit theoretical curve. The Julian day number is given, but the year must be inferred from the Orbit number. Orbits 3029 to 8330 were flown in 1970; smaller numbers refer to 1969 and larger orbit numbers to 1971. The quantity called electron flux is derived from the currents observed at large retarding potentials. When the value (cm^{-2} sec^{-1}) is followed by an asterisk it is proportional to the electron flux (greater than $\sim$10 ev) that is observed and the ion currents plotted have been corrected by an appropriate amount. The

absolute magnitude assigned to the flux is somewhat arbitrary and is based on the measured electron current per unit effective aperture area. The numbers are of qualitative value for satellite eclipse data (most of the data) in that they reveal the presence of conjugate photoelectrons when moving toward the magnetic equator and reflected conjugate photoelectrons when moving away from the magnetic equator. An estimate of the absolute electron flux of electrons with energy greater than 10 ev in particles/cm^2 sec ster assuming an isotropic flux can be obtained by dividing the printed number by π, if the "temperature" of these electrons is approximately 7 ev.

In addition, the presence of secondary electron fluxes at high latitudes (usually >60° dip) is commonly observed. This invariably signifies the presence of diffuse aurora in the absence of sunlight or conjugate electrons. The auroral fluxes are usually much more variable than photoelectron fluxes. When the flux value is greater than 9×10^6 cm^{-2} sec^{-1} but not followed by an asterisk this usually signifies the presence of Fe^+ ions (if the dip latitude is less than ~30°). For most of the data (but not all) the flux number is of the order 10^{-12} and in this case the number refers to a zero correction (in amperes) that has been made to the electrometer data before curve fitting or plotting (6×10^{-13} amps corresponds to a one bit correction; the electrometer noise level is of order 10^{-13} amp.).

The logarithmic ion current values have been obtained from an automatic ranging linear electrometer, and occasionally the deranging algorithm incorrectly adds or deletes a range change (a gain change of $\sqrt{10}$) resulting in an invalid ion characteristic curve. These curves are analyzed along with the rest, though they usually give larger σ values and error bars.

When the electrometer output is sampled while the electrometer is ranging the resulting data can be faulty. The program does not include the first point after a range change in the least squares analysis but does plot them with circles around them. For various reasons the data reduction program sometimes uses the wrong ion masses in the analyses, or incorrectly identifies an ion current region with the wrong ion mass. This results in invalid T_i, ψ, and N_i values. Most of the time these errors are readily recognized and the points are usually not plotted in SAT or SIGMA PLOTS because $\sigma > 10\%$.

There are two signals plotted during the duct period, the electrometer output and the duct amplifier output. The dots give the electrometer output, which is proportional to the total ion flux entering the RPA ($N_i V_s$). The magnitudes of the dot values have been normalized to unity at the beginning of each duct frame and fractions from 0 to 2 are plotted, though occasionally the actual values can exceed twice the initial value. Very large amplitude small scale structure is encountered where the instrument is completely aliased; changes in the electrometer sensitivity probably occur during these times but it is difficult to prove this. The continuous line joins points from the duct amplifier which have 1/3 the separation of the dots; this line shows variations from the initial ion concentration that can vary from +5% to -5%. Depending on the initial electrometer output voltage the duct amplifier may saturate at percentage changes smaller than $\pm 5\%$. This saturated condition is easily recognized.

The numbers (S's and Σ's) written at the top of the duct frames are derived values of irregularity scale size (S) and amplitude (Σ). The scale size S is derived from an algorithm which detects and counts peaks whose amplitude exceeds a certain threshold value above the previous minimum. The S values are given in units of km/peak. The parameters S_{11} and S_{12} are

derived from the amplifier output (continuous line) and refer to peaks >.3% and 1.0%, respectively. The parameters S_{21} and S_{22} are derived from the electrometer output and refer to peaks >3% and 10%, respectively. In practice, the S values have not been very meaningful, or useful.

The Σ values are given in dimensionless units corresponding to the RMS value of $\Delta N_i/N_i(\%)$. The parameters Σ_{11} and Σ_{12} are derived from the amplifier output, and refer to RMS percentage deviations from a horizontal straight line and a straight line joining the first and last points (before saturation), respectively. The parameters Σ_{21} and Σ_{22} are derived from the electrometer output (dots), and as before, refer to the RMS percentage deviations from a horizontal straight line and a straight line joining the first and last points, respectively. These Σ values are very useful in characterizing the relative smoothness (or roughness) of the ionosphere and they constitute the principal parameters of the Sigma plots.

At the top of each duct frame are given the electrometer sensitivity range for the maximum ion current in the previous ion sweep, together with the saturation electrometer voltage on that range at the start of the duct period. These quantities specify the ion current to which the duct electrometer plots have been normalized.

OGO PLOT

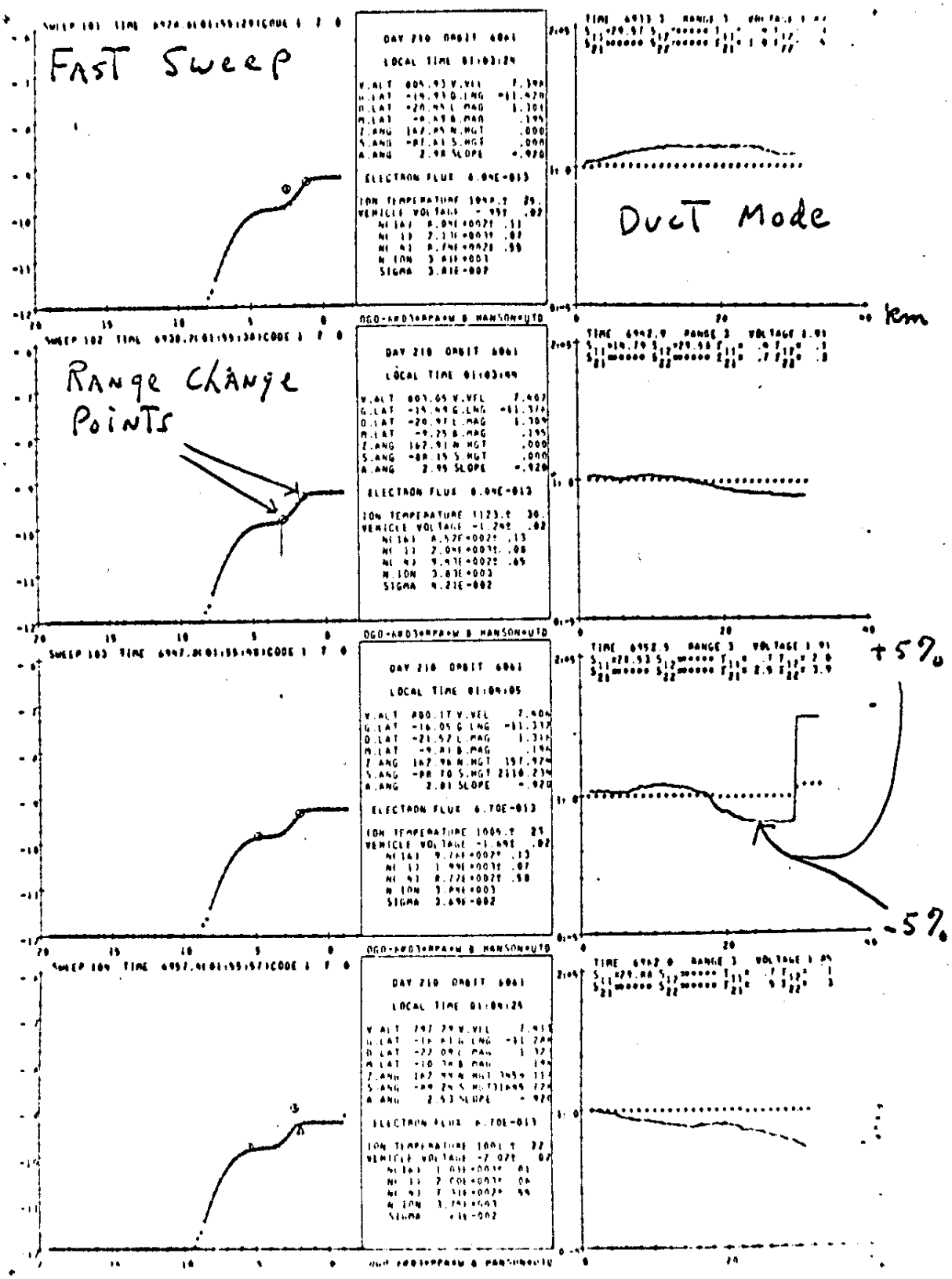

OGO PLOT

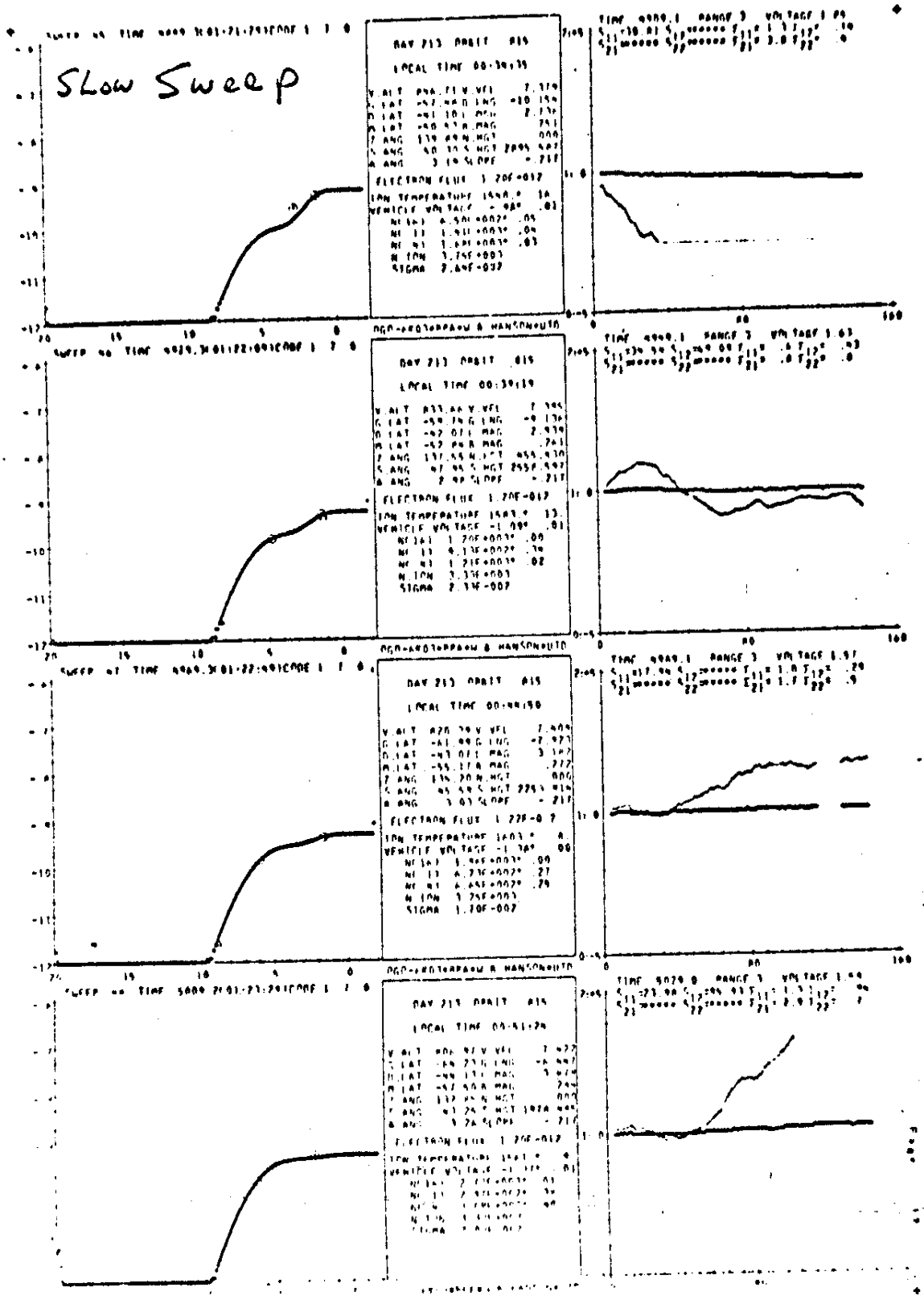

```
00000001000000010000004200000014000007B1000009E00000B090000001200000012000000 3A43432A1E4172656B0000  REC     1. LENGTH  3168
0001C231A0F2C26168C44187B77C259890D426DDBC9432A1F45431860F5C2364E1CC264FB3C4220663AC230F0E8C237A933
C224334DC22738F74044E31D411E29560000000100000C0100000001438098C414DC28F00000004C0E39586000000000B78C
1EA1C724E0CB396AC35743B0E95F41519DB14119EB854C8530E643B0EBC94119EB8500000004000000024193E835438A3D11
C13501050000000044204C64D000000004 3A5C1F60000000000000000442A626D424939DF3FEE64CD000000004312140400000
00004258588B000000000000000000000000010000002000000420000001400000 7B1000000 9E00000B1300000012000000 13
0000002743433D3641725A5700000001C2311 7E7C261477A411DB16CC259B92E426DDB0443474 4A443186429C235DD78C264
D6F4422006914 1ABF447C2372699C223AE83C226AE4740445B2B411DC77E000000020000000100000001438 13AF0414DC28F
00000004C0E39586000000000B785C026C72333AB396EAC0E43B188B341519DB1411AE148402B813743B18D0D411AE1470000
0004000000034 1365B8D4396AE2FC131ED1100000000441 77B264390EC32439EB9E900000000000000000442A75884 2396D0
3F801C330000000042CA7EA742BC39FD4229E8BE000000000000C000000001000000030000042000000140000078100000
009E00000B1D000000012C000001400000014434350 4F41725231000000012308ED9C261262F411FCA60C259E950426DDA62
0000000043186815C235ECD1C264B2AC421FA6E5424670FAC236AAB3C2233214C22623944043D336411D65A4000000030000
0001000000143B1DA48414DC28F00000C04C0E39586 0C000000B7820908C722395839714 7BA43B2280B41519DB1411B851F
4019BC4E43B22C0B411B851F0000000400000003411D2DB64394021FC12F2DD000000000441 7DF8F43A65A394399C5F30000
0000000000000442BE1C2421E79A13F4A6BED0C000000042748CD2426E0901421741 6B000000000000000000000000100000004
0000004200000014000 0C7B10000009E00000B2700000012000000150000000143436367417 24CFB00000001C23005CDC261
04E5411F672D4259E690426DD9E2000000004 3186CB4C234FC2DC2648E64421F473B42822127C236354EC222BD8BC22598E4
40434B44411D03CC0000C0040000000100000001 43B2799C414DC28F00000004C0E39586000000000B783A0A7C722A4A03972
99044 3B2C75F41519DB1411C28F6401E6A3543B2CB01411C28F60000000400000003411D46884 394B283C12D278A00000000
4418D09D43A98AD74394679600000000000000000442CAFC44212B1673F44CC9500000000427 1AC154269AF8E42155A5C0000
0000000000000000001C000000500000042000000140000078100000 9E00000B3100000012000000150000002A43437680
41724AB400000001C22F7CBFC260E39B411C6E194259B66E426DD9820000000043187206C2348B86C2646A1C421EE78FC2AA
2D24C235C633C2225074C2250E314042C34F411CA1F10000000500000000100000001 43B318F4414DC28F00000004C0E39586
00000000B77F61AAC721868A3975342843B366B74151 9DB1411C7AE14019DAC743B369FF411C7AE1000000040000000 3414A
835743B80C72C12BB1DEC000000044 19B29243A2BF29439281AA000000000000000000442D069F422D41D83FA1B41D00000000
43114968431000794232ABFC000000000000000000000001000000060000004200000014000007B10000009E00000B3B0000
0012000000160000001743438 99A41724B5D00000001C22EF3A9C260C24E4115D6CE4259864A426DD9420000000043187808
C2341ADAC26445D2421E87DEC26E785DC2355D35C221EA6BC22483774042 3B52411C401200000006000000010000000143B3
B855414DC28F00000004C0E39586000C00000B776E3B0C71F4A5F39767B5C43B406174 1519DB141 1CCCCD40A6C53443B408F4
411CCCCD000000040000000 34136A8C3438BDA69C12A0E62000000000441A02AE43B38376438ABAA1000000000000000000442D
E69042221EB03F7991 1C000000042CFCBC942C1D1434224 08B400C000000000000000000000001000000070000004200000014
000007B10000009E00000B4500000012000000170000002434 39E2F4172458500000 1C22E6873C260A35A411680154259
5588426DD730432F5913431 87A01C233A98FC264246D421E2955C231E1B5C234DEAFC22170CCC223F6BF4041B547411BE6B4
0000000700000001000000 0143B45A13414DC28F00000C04C0E39586000000000B785C026C72333AB3977D9EA43B4A7D64151
9DB1411D1EB8401 1DAA643B4AA40411D1EB8000000004000000003412E2F7743938089C13298CA000000004 41AEB6B43AB911E
438878DB000000000000000000442E2C0A421E066C3F67FC430000000042AB1D9A42A37A15421DFCFE0000000000000000000000
0001000000080000004200000014000007B10C00009E00000B4F0000001200000017000002743 43AB1841723B3F00000001
C22DDF3EC260871541 1C1DCE4259259442 6DD3B243538F9F43187 8B2C2333AC8C264063A421DCE39419CC4C8C2345418C220
ED3DC2236C304041345841 1B967A000000080000000100000001 43B4F967414DC28F00000004C0E39586000000000B7818129
C72215953977D5AB43B5472A4 1519DB1411D1EB840BC618E43B54E84411D1EB8000000040000000 3412E7C7C4391C1BAC131
0323000000004 41B7F2343A5D781438591 8B0C000000000000000442E35B4421E689B3F684E91000000042AD9ECE42A2B907
421D6F950000000000000C000000010000000900000042000000 1400000078100000 9E00000B590000012000000180000
000F4343BB01417233E6C000000 1C22D5606C2606ACF411E5DDD4258F59E426DD03F000000004 31877DDC232CC00C263E806
421D731842457BD7C233CFF0C2207157C222E19D4040B365411 8463F000000090000000100000001 43B598BF414DC28F0000
0004C0E39586000000000E77CBA4CC720D3BD39792096 43B5E6824 1519DB1411DC28F4019CE7B43B5EA82411DC28F00000004
0000000341184F9E43 9354D2C12E9DF700000000441CAE3943A560BE43826041000000000000000000442F2A4941FDD7B03F35
8DBA000000004 25AAE8942552F2C41EE82E2000000000C000000000000001000000 0A000000420000001400000 7B10000009E
00000B6300000012000000 1800000344343CAE941722F7A000000 1C22CCCD2C2604E8B411E04044258C5AA426DCCD50000
0000431877 80C2325D39C263C9D3421D1800428129D5C2335202C21FFC82C222570D4040327641 1AF6050000000A00000001
0000000143B6381341 4DC28F00000004C0E39586000000000B77D422BC720F77F397A70CF43B685D641519DB1411DC28F4045
191443B6897841 1DC28F0000004000000034121EF334391671 7C12D0B480000000044 1CF31343A4879E4380376000000000
00000000442F3F0342155CDC3F4A1D7D000000004 27DB27742751 03B42145D57000000000000000000000010000000B0000
0042000000140000078 1C000009E00000B6D0000001200000019000000 1C4343DAD241722DFC00000001C22C439AC2603245
411AF69B425895B3426DC97300000000431877 99C231EE71C263AB9F421CBCE2C2AB269DC232DA1FC21F8EE5C221CC7A403F
B183411AA5C900000008C000000100000001 43B6D76B414DC28F00000004C0E39586000000000B77A12EEC72020EF397BBD52
43B7252E41519DB1411E147B40371E7943B72875411E147B00000C040000000 3412E4056438F91A9C12B49AC00000000441D
DEDF43A08D67437D85A7000C000000000000442FC0104217AE243F513B800000000428C80EE4281CEC242160A8800000000
0000000000000001000C00C0000004200000014000007B1 0000C09E00000B7700000012000000 1A000000054343EABC4172
2F6C00000001C22BBA5BC26015FE411402 4F425865B8426DC617000000004 3187825C2317FA2C2638D6A421C618FC26F7401
C232681BC21F2794C22141E0403F308A411A5589000000C00C000000100000001 43B776CB414DC28F00000004C0E395860000
0000B774C431C71EBB543 97BB80343B7C48E41519DB1411E6666402A7EE443B7C768411E6666000000040000000 3411E769E
43904BFAC129C50F00000000441E92F3439D61A7437C4674000000000000000044302D754212F6CB3F3F8434000000004271
09CE42666ECB42112A11C000C00000000000
0000000100000000D000000420C000014000007B100C0009E00000B810000001200000 1A000000284343F91341722A920000  REC     2. LENGTH  3168
```

D-20504

C-16933

20-814

6/07/69 - 8/01/69

256

```
0001C2360F5542A6834C411F9581421CE79B42491C160C0000000C000000C23700A542A5F3C04240B99642B1958DC24C4BAD
C241BAF4C23B24D040827860414E31E8000000360000000000000045151 7C14213D0E500000006C03796B400000000000
0000000000003A3EB3FD41FE51EA4214733341194 7AE4019FCE7451519014119 47AE000000060C0000000000000000000000
0000000000000000000C0000000000000000000000C000000000C0000000000000000000000C0000000000000000000000
0000000000000000000C0000000000C0001000105E6C000002F0000032E000007B1000000D500000024000000B00000003
0000002043 1E1283417C4703000000 1C23388A242A74F2E41282BDC42138F694246846A0000000000000000C234979842A6
BFC7423E895A42369779C24E3236C23E23FAC2389763408138F641424DB2000000360000000000004224136B64213D0E5
00000006C03796B400000000000000000000000003A3F7F2E4237E49B42147333411 9999A40AAE6154515 1B824119999900000
0006000000000000000C0000000000000000000000000000000000C0C0C000000000000000000C0000000000000000000000
0000000000000000000000C0000000000000000000000000000000000000000000000000000 1000105B700000C2F0000032E000007B10000
00D50000004C0000000BC0000007000000074 31D79AE417C7262C0000001C230FD8D42A808F141250D7A421623B24243E925
0000000000000000C2322A5342A77A48423C4787C2438D4DC24963DFC23B2DFCC236069F407FC61E413872F400000360000
0000000000424C2AC0421 3D0E500000006C03796B400000000000000000000003A69903D425FFBA542147333411CCCCD
40C3AAB44515 1E02411CCCCD0000000600000000000000000000000000000000000000000000000000000000000000000000
0000000000000000000C0000000000000000000000000000000000000000000000000000000000000000000000000000000 10010 5B8
0000002F0000032E0000C7B1000000D5000000740000000B00000C0A000000 15431CE8C1417CA2100000000 1C22E722F42A8
AD34411BA487421 8B13B424 14F1400000000000000000C22FBD2842A81F564239F5BA42A98A87C247A39AC2386C84C23376C7
407E19CF4130C9A3000000360000000000000004274122C4213D0E50C000006C03796B400000000000000000000003A54
ED4E4287E31 1421 4733341 1EB8524058 3B9F4515208141 1E666600000060000000000000000000000000000000000000
0000000000000000000C0000000000000000000000000000000000000000000000000000000000000000000000000000000
0000000000000000001C00105B90000002F0000032E000007B1000000D50000009C0000000B0000000D0000000D431C6336
417CB8DF00000001C22BE0FE42A93A15412564 7D421B59F9423EB13E422B74BB00000000C22D4BAF42A8AD5B4237888A422F
948AC2455BCAC235016BC230E27340 7C1869412B2291C0000036E0000000000429C11A94213D0E500000006C03796B4
0000000000000000000C0C0003A49D0A642AFE28E42147333411E147B4095FAE34515230 1411DC28F000000600000000000
0000000000000000000000C0000000000000000000000C0000000000000000000000000000000000000000000000000000000
0000000000000000000C0C0000000000000000000000000000 1000105BA0000002F0000032E000007B1000000D5000000C40000
000B0000000F000000374 31BE483417CDD1D00000001C2294DAE42A9BC2E4122 1305421DF42C423C11C4000000000000000
C22AD98542A9307D4235CDE7C24A344FC2434375C2320879C22E4C9F4079EA8041264B2400000036000000000000042C4
1126421 3D0E500000006C03796B400000000000000000000003A49057542D7E20B4214733341 1D70A440AB6D1A45152582
411D70A400000006000 0CC0000000000000000000000000000000000000000000000000000000000000000000000000000
0000000000000000000000C0000000000000000000000000000000000C0000000C0000000000000000000000 1000105BB0000002F0000032E
000007B1000000D500C0CCEC0000000B0000001200000C19431B6E1B417D0580000000 1C226B7F342AA32144117AC9A4220
8BA0423970B1000000000C0000000C22866D142A9A7324232837B42A432F1C241296CC22F3544C228B5 10407787F7412254DC
0000003600000000000C0000042EC101F4213D0E50C0C0006C03796B4C000000000000000000003A4E93C942FFE1044214
7333411FAE14407 8656A45152800412C0000000000060000000000000000000000000000000000000000000000000000
0000000000000000000C0C0000000000000C0000000C0000000000C0000000000000000000000000000000000000000000
0001000105BC0000002FC0000032E00000 7B1000000D50000C1140C00000B0000001400000024431B04E6417D146700000001
C2241F0042AA9999412 2CCCE422335BC4236CDA942C2B139000000C225F55242AA0EE6422FE3EA422AD99BC23E88FDC22B
E36AC2291B1B4074DB0F411F4646000000360000000C0000000431140F94213D0E500000006C03796B4000000000000000
00000003A69903D43127EC0E42147333412 1EB85412EB1BE45152A804121E885000000060000000000000000000000000000
0000000000000000000C0000000000000000000000000C0C0000000C0000000000000000000000000000000000000000000
0000000000000000000C00C0000000 1000105BD0000002F0000032E000007B1000000D5000001 3C0000000B0000001600000
0035431AA34C417D30B7C0000001C221847842AAFA7C411F7558 4225D5174234295800000000C223859C42AA6F73
422D3A97C24E6293C23C02E2C228E800C2267FF240720 7FC411C99EA0C0000360000000000000004313C0F54213D0E50000
0006C03796B400000000C0000000000000003A60D5264314FE04421473334124CCCD4116F4A545152D014124CCCD00000006
0000000000000000000C0000000000000000000000000000000000000000000000000000000000000000000000000000000
0000000000000000000C0000000000000000000000000000000000000000000000000000 1000105BE0000002F0000032E000007B1000000D5
0000016400000000B00C0001E000000394 31A4AE6417D50F600000001C21EE83142AB53D2411403454228724C423183C90000
0000000000000C2211872 42AAC7C3422A864042A07A7FC2396C7EC2260B74C223E376406F0837411A5A5400000036000000000
0000000043 1640E14213DCE50C000006C03796B4000C0000000000000000003A5C120343177DEF421473334125 1EB84111
AA7F45152F8141251EB8C00C0CC6000000000000000000C0000000C0C0000000000000000000000000000000000000000000
0000000000000000000C0000000000000000000000000000000000000000000000000000000000000000000000000000000
0000000000000000000C0000000000000000000000000000000000000000000000000000000000000000000000000000000
0000000000000000000C0000000000000000000000000000000000000000000000000000 1000105BF0000
002F0000032E000007B1CC0C00D5000001 8C0000000E0000001A0000003443 1A00EA417D5746000000 1C21C499342ABA427
4120D5C3422B1D7942 2EDCAB431D62140C000000C21EB22E42AB158F4227C8AB42278298C23646E1C222CEE8C2214523406B
CF9841189255000000360000000000000004318C0DD4213D0E50C000006C03796B4000000000000000000003A68C50C
4319FDEB4214733341 2A3D7141156437451532004 12A3D7100C0000060000000000000000000000000000000000000000
0000000000000000000C0C0C0000000000000000000000000000000000000000000000000000000000000000000000000000
0000000000000001000 1C5C00000002F0000032E00000 7B1000000D5000001B40000000B0000001C0000002C4319BF26417D
6AFA00000001C219A9E542ABF04E411D74ED422DC053422C34AE0C0C0000000000C21C518442AB5E1042250AEBC251660F
C2332B09C21FD8DEC21EA5FC40687E984116FF6C0000003600000000000000431B40D44213D0E500000006C03796B40000
0000000000000000000 3A60D526431C7DE3421473334125 1EB84018DF1E45153480412 51EB8000000060000000000000000
0000000000000000000C0000000000000000000000000000000000000000000000000000000000000000000000000000000
0000000000000000000C0C000C000C000C0000
0000000 1000105C10000C02F0000032E000007B1000000D5000001DC0000000E0000001E0000001E4319874B417D82710000  REC      5, LENGTH  2376
0001C21709094 2AC37B541112D96423061764229 8BD400000000000000C219F8C342ABA06442224E71429DBFB2C22FEFDB
```